Front. Environ. Sci. Engin. China 2008, 2(4): 397–409
DOI 10.1007/s11783-008-0074-0

RESEARCH ARTICLE

# Fenton process for degradation of selected chlorinated aliphatic hydrocarbons exemplified by trichloroethylene, 1,1-dichloroethylene and chloroform

**Zhimin QIANG[1], Weiwei BEN[1], Chin-Pao HUANG (✉)[2]**

1 Research Center of Eco-Environmental Sciences, Chinese Academy of Sciences, Beijing 100085, China
2 Department of Civil and Environmental Engineering, University of Delaware, Newark, DE 19716, USA



**Abstract** The degradation of selected chlorinated aliphatic hydrocarbons (CAHs) exemplified by trichloroethylene (TCE), 1,1-dichloroethylene (DCE), and chloroform (CF) was investigated with Fenton oxidation process. The results indicate that the degradation rate was primarily affected by the chemical structures of organic contaminants. Hydroxyl radicals (·OH) preferred to attack the organic contaminants with an electron-rich structure such as chlorinated alkenes (i.e., TCE and DCE). The dosing mode of Fenton's reagent, particularly of $Fe^{2+}$, significantly affected the degradation efficiency of studied organic compound. A new ''time-squared'' kinetic model, $C = C_o\exp(-k_{obs}t^2)$, was developed to express the degradation kinetics of selected CAHs. This model was applicable to TCE and DCE, but inapplicable to CF due to their varied reaction rate constants towards ·OH. Chloride release was monitored to examine the degree of dechlorination during the oxidation of selected CAHs. TCE was more easily dechlorinated than DCE and CF. Dichloroacetic acid (DCAA) was identified as the major reaction intermediate in the oxidation of TCE, which could be completely removed as the reaction proceeded. No reaction intermediates or byproducts were identified in the oxidation of DCE and CF. Based on the identified intermediate, the reaction mechanism of TCE with Fenton's reagent was proposed.

**Keywords** Fenton's reagent, trichloroethylene, 1,1-dichloroethylene, chloroform, degradation, dechlorination

## 1 Introduction

Chlorinated aliphatic hydrocarbons (CAHs) are prevalent groundwater contaminants and significant components of hazardous wastes and landfill leachates. Most CAHs released from industrial, commercial, and agricultural sources are chlorinated alkanes and alkenes that contain between one and three carbon atoms [1]. Chlorinated alkenes are commonly used as cleaning solvents in dry-cleaning operations and semiconductor manufacturing. Chlorination is a widespread industrial practice because it yields compounds of low flammability, high density, high viscosity, and improved solvent properties compared to non-chlorinated solvents [2]. In the 1970s, 46.5% chlorine gas was used for the production of chlorinated organic compounds in the United States [3]. Chlorinated solvents are used mainly for degreasing and cleaning a great variety of products, from machine parts to computer chips. Trichloroethylene (TCE) is an excellent solvent for a large number of natural and industrial materials. It is moderately toxic, nonflammable, and slowly oxidizable in the air. TCE has the greatest use in vapor degreasing of fabricated metal parts [3]. Chloroform (CF) has been used most frequently as a dry-cleaning spot remover and as a degreasing agent for machine and engine parts. Other applications include industrial intermediates, insecticides, and the purification of vitamins. The properties of chlorinated solvents that render them mobile in groundwater systems include high density, relatively high water solubility, and low biodegradability [2]. A survey of 7000 wells conducted in California from 1984 to 1988 showed that approximately 1500 had detectable concentrations of organic chemicals present. The most common chemicals detected were chlorinated hydrocarbons such as tetrachloroethylene (PCE), TCE, CF, 1,1,1-trichloroethane, and carbon tetrachloride [4]. In addition, at the National Priorities List (NPL) sites the contaminants that are most frequently found include TCE (42%) and PCE (28%) [5]. Consequently, CAHs are listed among the eight major classes of priority pollutants by the US Environmental Protection Agency (EPA) [6].

Received August 6, 2008; accepted September 8, 2008

E-mail: huang@ce.udel.edu

CAHs have been treated using biological, physical, and chemical processes. El-Farhan et al. [7] investigated the cometabolization of TCE with toluene using laboratory soil columns. It was observed that while toluene was fully biodegraded, a substantial amount of TCE was not degraded because it diffused faster and had slower transformation rates than toluene. Though biological processes might degrade chlorinated solvents by cometabolizing with another organic compound, the degree of mineralization is very low. Furthermore, the byproducts produced may be more toxic than parent compounds.

Physical processes including thermal-enhanced soil vapor extraction (SVE) have been employed to effectively remediate the soils contaminated by chlorinated solvents. Heron et al. [8] heated a silty, low permeable soil contaminated by TCE using electric current to enhance soil vapor extraction. They achieved 99.8% mass removal at 85–100°C after 37 d. Kawala and Atamanczuk [9] applied microwave radiation (600 W, 2450 MHz) heating to remediate soils contaminated by several volatile and semi-volatile organic compounds. TCE concentration was decreased in the heated zone from 2.2% to about 0.01% (mass%) after the first 24 h. Although fast and effective, the thermal-enhanced SVE process is energy consumptive.

The chemical processes applied to treating chlorinated solvents include chemical reduction using zero-valent metals or vitamin $B_{12}$, and advanced oxidation processes (AOPs) using Fenton's reagent, UV/$TiO_2$, electron beam, and ultrasound [10]. Burris et al. [11] investigated the reductive dechlorination of PCE, TCE, *cis*-DCE, and vinyl chloride (VC) catalyzed by vitamin $B_{12}$ using Ti [III] citrate as a bulk reductant in a vapor/water batch system. They reported that the reductive dechlorination proceeded very slowly, and many partially dechlorinated compounds were formed as the terminal byproducts. Ho et al. [12,13] employed a Lasagna process, which integrated electro-osmosis with Fe(0) reductive dechlorination, for in-situ remediation of a TCE-contaminated clay site in Paducah, Kentucky. Their results indicated that the treatment effectiveness varied with location, but 95%–98% of TCE could be removed in the contaminated areas bracketed by iron filing treatment zones. Gotpagar et al. [14] examined the reductive dechlorination of TCE with Fe(0). They reported that the amount of TCE degraded at any time was directly proportional to the dissolved iron in the solution, and the iron surface area was a crucial factor in controlling TCE degradation. The removal efficiency of total organic carbon (TOC) lagged behind that of TCE, suggesting the formation of partially dechlorinated compounds. Arnold and Roberts [15] studied the degradation of chlorinated ethylene with Zn (0), and found that the reaction rate increased with increasing degree of chlorine substitution, i.e., *trans*-DCE < TCE < PCE. The reaction of *trans*-DCE with Zn (0) was very slow ($t_{1/2} > 125$ d), and acetylene, ethylene and VC were identified as major byproducts. The reduction of TCE produced *trans*-DCE, acetylene, and *cis*-DCE as major byproducts, and VC, ethylene and 1,1-DCE as minor products.

AOPs have also been applied to degrading chlorinated solvents. Cooper et al. [16] investigated the degradation of TCE in aqueous solution at a large scale (400 L/min) using high-energy electrons generated by $^{60}Co$ $\gamma$ irradiation. TCE was degraded effectively and a complete chloride release was obtained. Aldehydes and formic acids were the major reaction byproducts, and no partially dechlorinated compounds were detected. In the electron-beam irradiation process, both oxidation (from ·OH) and reduction (from electron and hydrogen radicals) contributed to organic removal. Bhatnagar and Cheung [17] investigated the ultrasonic destruction of chlorinated volatile organic compounds in water. The aqueous solutions of methylene chloride, CF, carbon tetrachloride, 1,2-dichloroethane, 1,1,1-trichloroethane, TCE, and PCE at concentrations of 50–350 mg/L were irradiated with 20-kHz ultrasonic waves (0.1 kW/L) under ambient temperature and pressure conditions. The organic concentrations decreased rapidly and the percent destruction varied from 72% to 99.9%. Gas chromatography/mass spectrometry (GC/MS) analysis indicated that no other chlorinated byproducts were formed in ultrasonication. Crittenden et al. [18] studied the photocatalytic oxidation of chlorinated hydrocarbons in water using UV and $TiO_2$ whose surface was modified with platinum or silver. TCE was totally mineralized to $CO_2$ and HCl. Ollis et al. [19] reported that the chlorinated hydrocarbons including PCE, dichloroethane, monochloroacetic acid (MCAA) and dichloroacetic acid (DCAA) were completely mineralized by photoassisted heterogeneous catalysis with the aqueous slurry of near-UV illuminated $TiO_2$. It was also reported that doping a non-precious metal oxide catalyst ($RuO_2$) on $TiO_2$ could effectively enhance the degradation efficiency of TCE in aqueous phase under near-UV illumination [20]. However, Glaze et al. [21] identified several chlorinated terminal byproducts from the degradation of TCE with UV/$TiO_2$. At neutral pH and under atmospheric air, a low yield of dichloroacetaldehyde (< 4% based upon TCE degraded) and DCAA was observed together with a trace amount of trichloroacetaldehyde and TCAA. It is noted that DCAA is a known animal carcinogen and its potency is greater than that of TCE [22]. Ravikumar and Gurol [23] investigated the degradation of TCE in the presence of sand by the Fenton's reagent and reported that 90% of the chloride was released from TCE. Chen et al. [24] applied Fenton's reagent to in-situ remediation of TCE-contaminated soil column. They found that Fenton's reagent was able to oxidize more than 93% of dissolved TCE in groundwater and more than 98% of TCE in soil slurries. Tang and Huang [25] reported that 80% of chloride was released from the oxidation of TCE by the Fenton's reagent. Tang and Tassos [26] examined

the oxidation of trihalomethanes, such as bromoform and CF, using the Fenton's reagent, and found that though bromoform was readily degradable, CF was very difficult to degrade. More recently, the thermally activated persulfate oxidation process, which utilizes highly reactive sulfate radicals ($SO_4^{\cdot -}$) as indirect oxidants, has been investigated for degradation of TCE at pH 7 and temperature 40°C in aqueous phase [27].

As described above, AOPs can remove CAHs more effectively than biological and chemical reduction processes. This study aims to improve the degradation efficiency of selected CAHs (i.e., TCE, DCE, and CF) with the Fenton's reagent through modifying the dosing mode of $H_2O_2$ and $Fe^{2+}$. In addition, the degree of dechlorination was examined and potential reaction mechanism was proposed.

## 2 Materials and methods

### 2.1 Chemicals

TCE (spectrophotometric grade, > 99.5%), DCE (ACS reagent grade, 99%), and CF (HPLC grade, > 99%) were purchased from Sigma-Aldrich (Milwaukee, WI, USA). $H_2O_2$ (31.5% w/w) and $FeSO_4$ (98%) were purchased from Fisher Scientific (Pittsburgh, PA, USA). The major physico-chemical properties of selected CAHs are summarized in Table 1 [28]. TCE and DCE have an unsaturated double-bond structure, and their water solubility and vapor pressure increase with the descending degree of chlorination. CF has a saturated and highly chlorinated structure, high water solubility, and moderate vapor pressure, in comparison with TCE and DCE.

**Table 1** Major physico-chemical properties of selected CAHs [28]

| property | TCE | 1,1-DCE | CF |
|---|---|---|---|
| molecular formula | $CHCl=CCl_2$ | $CCl_2=CH_2$ | $CHCl_3$ |
| molecular weight | 131.5 | 97.0 | 119.4 |
| water solubility/mg·L$^{-1}$ at 25°C | 1100 | 2500 | 9300 |
| vapor pressure/mmHg at 20°C | 60 | 500 | 160 |
| log$K_{ow}$ at 25°C | 2.42 | 2.02 | 1.93 |

The reaction solution of selected CAHs with a desired concentration was freshly prepared by dissolving a target organic compound in distilled water in a well-sealed glass flask. The stock solutions of $H_2O_2$ and $FeSO_4$ were prepared weekly in which sulfuric acid was purposely added to retard the decomposition of $H_2O_2$ to $O_2$ and the oxidation of $Fe^{2+}$ to $Fe^{3+}$.

### 2.2 Reaction system

The laboratory setup of the reaction system is illustrated in Fig. 1. The oxidation of selected CAHs was carried out

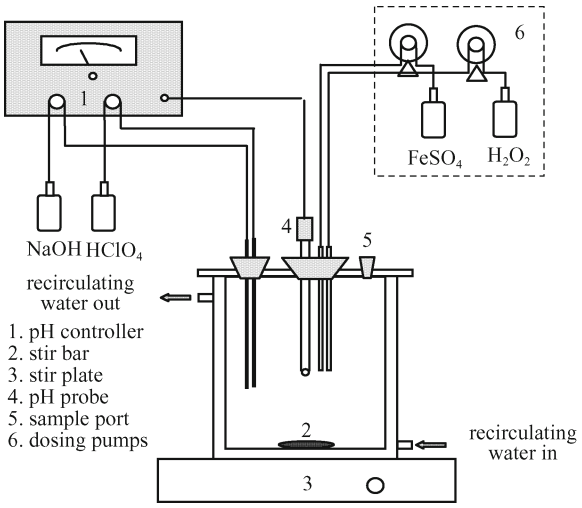


**Fig. 1** Schematic diagram of reaction system for degradation of selected CAHs with Fenton oxidation process

in a double-jacketed glass reactor with an effective volume of 600 mL. The reactor was filled with reaction solution and closed to prevent the volatile loss of organic solute. The reaction solution was completely mixed by a magnetic stir plate. A pH controller (Model pH-40, New Brunswick Scientific Co., NJ, USA) was used to maintain a constant solution pH by intermittently adding NaOH (1.0 mol/L) or $HClO_4$ (1.0 mol/L). Default experimental conditions were ambient room temperature (23°C), 0.05 mol/L $NaClO_4$ of ionic strength, and pH 3, unless otherwise stated. $HClO_4$ was used for pH adjustment instead of HCl based on two considerations: (a) $Cl^-$ is an ·OH scavenger, and (b) HCl interferes with the analysis of $Cl^-$ released from the dechlorination of selected CAHs.

### 2.3 Analytical methods

All selected CAHs were analyzed by gas chromatography/electron capture detector (GC/ECD) (Model 5890, Series II, Hewlett Packard, CA, USA) with nitrogen carrier gas. An HP-5MS capillary column (crosslinked 5% Ph Me Silicone, 30 m × 0.25 mm × 0.25 μm film thickness) was used for organic separation. Oven temperature was held at 50°C for 5 min for each sample analysis. Other instrumental conditions were GC injector temperature of 250°C, ECD detector temperature of 300°C, column head pressure of 125 kPa, and a total flow rate of 80 mL/min.

GC/MS (GC Model 5890, MS Model 5972, Hewlett Packard, CA, USA) was used for the identification and quantification of intermediates and byproducts with an HP-5MS capillary column. The oven temperature program was set as follows: started at 50°C and held for 2 min, ramped at 5°C/min to 100°C and held for 2 min, and ramped at 10°C/min to 240°C and held for 2 min. The total analysis time for each sample was 30 min. The

injector temperature was 180°C and the detector temperature was 280°C. A five-milliliter sample was taken and extracted with 5 mL of hexane. Sodium hydroxide (10 μL, 1.0 mol/L) was added to adjust the pH of the aqueous layer to about pH 11. The pH adjustment terminates ·OH reactions, and dissociates intermediate carboxylic acids to prevent partial extraction by hexane. The parent compounds in the hexane layer were determined by GC/ECD as mentioned above. The remaining aqueous layer and a thin hexane layer were purged by nitrogen gas for 10 min. Nitrogen purge would remove the hexane layer and the remaining CAHs as well, thus minimizing the interference with the analysis of intermediates and byproducts. The aqueous layer was then acidified to about pH 0.5 by $HClO_4$ (5.0 mol/L). The $pK_a$ values of mono-, di-, and tri-chloroacetic acids which are possible intermediates are 2.87, 1.26, and 0.52, respectively. At pH 0.5, most of these carboxylic acids are present in neutral forms that are more extractable by organic solvent.

Methyl *tert*-butyl ether (MTBE) was used for carboxylic acids extraction. MTBE (2.5 mL) was added to the acidified aqueous layer. After vigorous shaking, the MTBE layer was taken out and derivatized by diazomethane using a Fales diazomethane generator [29] manufactured by Wheaton Scientific (Millville, NJ, USA). The reagent used for diazomethane generation was 1-methyl-3-nitro-1-nitrosoguanidine (MNNG, 97%) purchased from Sigma-Aldrich (Milwaukee, WI, USA). The derivatization procedure modified from Knapp [30] is described as follows: 2.5 mL of MTBE extract was added to the outside tube of the diazomethane generator; 132 mg of MNNG reagent and 0.5 mL of distilled water (for heat dissipation) were added to the inside tube; 0.6 mL of 5.0 mol/L NaOH was slowly injected to the inside tube through a Teflon rubber septum via a syringe with a narrow gauge needle to initiate the generation of diazomethane. Derivatization was completed if a yellow color persisted in the solution. The derivatized MTBE solution was then analyzed by GC/MS in comparison with authentic organic compounds. Caution should be taken because diazomethane is explosive. Derivatization was carried out in an efficient hood and behind a safety shield. The lower part of the generator was immersed in an ice bath to dissipate reaction heat and reduce the volume of diazomethane gas.

The concentrations of $H_2O_2$ and $Fe^{2+}$ were determined by measuring the light absorbance after chelating with certain reagents using an HP diode array spectrophotometer (8452A) at 410 nm and 510 nm, respectively [31]. Chloride concentration was analyzed using a chloride-selective electrode (Model 94-17B) coupled with a reference electrode (Model 90-02) from Orion Research Inc. (Boston, MA, USA). The two electrodes were connected to a Corning pH meter (Model 125, Corning, NY, USA) which recorded the redox potentials. Total organic carbon (TOC) was analyzed by a Tekmar-Dohrmann TOC analyzer (Model DC-190, Mason, OH, USA).

## 3 Results and discussion

### 3.1 Dosing modes of Fenton's reagent

The Fenton oxidation process is a competitive reaction system. Organic contaminants, $H_2O_2$, and $Fe^{2+}$ all compete for ·OH. The dosing mode of the Fenton's reagent determines the time-dependent concentrations of $H_2O_2$ and $Fe^{2+}$, thus affecting the degradation kinetics of studied organic compounds. If $H_2O_2$ is singly dosed, there is initially an excess amount of $H_2O_2$ which stresses its competition for ·OH. Likewise, if $Fe^{2+}$ is singly dosed, the initial excessive $Fe^{2+}$ will significantly compete for ·OH. The second-order rate constants of $H_2O_2$ and $Fe^{2+}$ towards ·OH are $2.7 \times 10^7$ $(mol/L)^{-1}\cdot s^{-1}$ and $3.2 \times 10^8$ $(mol/L)^{-1}\cdot s^{-1}$, respectively [32]. It is seen that $Fe^{2+}$ scavenges ·OH approximately one order of magnitude faster than $H_2O_2$. As a result, the dosing mode of $Fe^{2+}$ is expected to influence the degradation kinetics of studied organic compounds more prominently than that of $H_2O_2$. To minimize the competition of $Fe^{2+}$ for ·OH, two dosing modes (i.e., a pseudo-continuous dosing mode and a continuous doing mode) were examined for the degradation efficiency of selected CAHs in this work. In the pseudo-continuous dosing mode, $H_2O_2$ was dosed in batches at the beginning of the reaction while $Fe^{2+}$ was continuously dosed. In the continuous dosing mode, both $H_2O_2$ and $Fe^{2+}$ were continuously dosed throughout the course of reaction.

### 3.2 Kinetic model development

The intrinsic reaction kinetics of an organic compound towards ·OH is generally described by a second-order expression:

$$-\frac{d[\mathrm{RH}]}{dt} = k_{\mathrm{int}}[\mathrm{RH}][\cdot\mathrm{OH}], \quad (1)$$

where RH represents the organic compound and $k_{\mathrm{int}}$ is the second-order intrinsic rate constant. Most of the $k_{\mathrm{int}}$ data have been supplied by radiation chemists [32]. In contrast to other oxidants, the reaction of ·OH with organic compounds containing unsaturated structures generally proceeds with a rate constant approaching the diffusion-controlled limit ($\sim 10^{10}$ $(mol/L)^{-1}\cdot s^{-1}$). Many researchers [33,34] have proposed pseudo-first-order kinetics for the oxidation of organic compounds by the Fenton's reagent, with batch dosing of $Fe^{2+}$ and continuous dosing of $H_2O_2$. In those cases, a steady-state assumption for ·OH was applied. If the concentration of ·OH remains nearly constant during the course of reaction, a pseudo-first-order

kinetic expression (Eq. (2)) can be readily obtained by transforming Eq. (1):

$$-\frac{d[\mathrm{RH}]}{dt}=k_{\mathrm{obs}}[\mathrm{RH}], \tag{2}$$

$$k_{\mathrm{obs}}=k_{\mathrm{int}}[\cdot\mathrm{OH}], \tag{3}$$

where $k_{\mathrm{obs}}$ is the observed rate constant ($\mathrm{min}^{-2}$). It is clear from Eq. (3) that the observed rate constant, $k_{\mathrm{obs}}$, depends on both $k_{\mathrm{int}}$ and ·OH concentration. Though $k_{\mathrm{int}}$ is very large, $k_{\mathrm{obs}}$ is by far smaller due to an extremely low concentration of ·OH in the reaction system. In natural water systems, ·OH is produced by photolysis of nitrate ions with a concentration usually ranging from $10^{-18}$ to $10^{-16}$ mol/L [28]. From the viewpoint of practical application, $k_{\mathrm{obs}}$ is more useful than $k_{\mathrm{int}}$ because the ·OH concentration varies markedly in different reaction systems.

However, the ·OH concentration is no longer constant in pseudo-continuous and continuous dosing modes where $Fe^{2+}$ is continuously supplied to the reactor. Either $H_2O_2$ or $Fe^{2+}$ may accumulate in the reaction system, thus increasing the formation rate of ·OH. Our previous work has shown that the ·OH concentration approximately increases as a linear function of reaction time, i.e., $[\cdot\mathrm{OH}]=at$ [31]. Consequently, Eq. (1) is changed to:

$$-\frac{d[\mathrm{RH}]}{dt}=ak_{\mathrm{int}}t[\mathrm{RH}]. \tag{4}$$

Integration of Eq. (4) leads to:

$$[\mathrm{RH}]=[\mathrm{RH}]_{\mathrm{o}}\exp\left(-k_{\mathrm{obs}}t^{2}\right), \tag{5}$$

$$a=2k_{\mathrm{obs}}/k_{\mathrm{int}}, \tag{6}$$

where $a$ and $[\mathrm{RH}]_{\mathrm{o}}$ represent the slope of ·OH concentration increment (mol/L·$\mathrm{min}^{-1}$) and the initial concentration of organic compound (mol/L), respectively. The value of $k_{\mathrm{obs}}$ can be readily obtained by fitting the experimental data with the developed "time-squared" kinetic model (Eq. (5)).

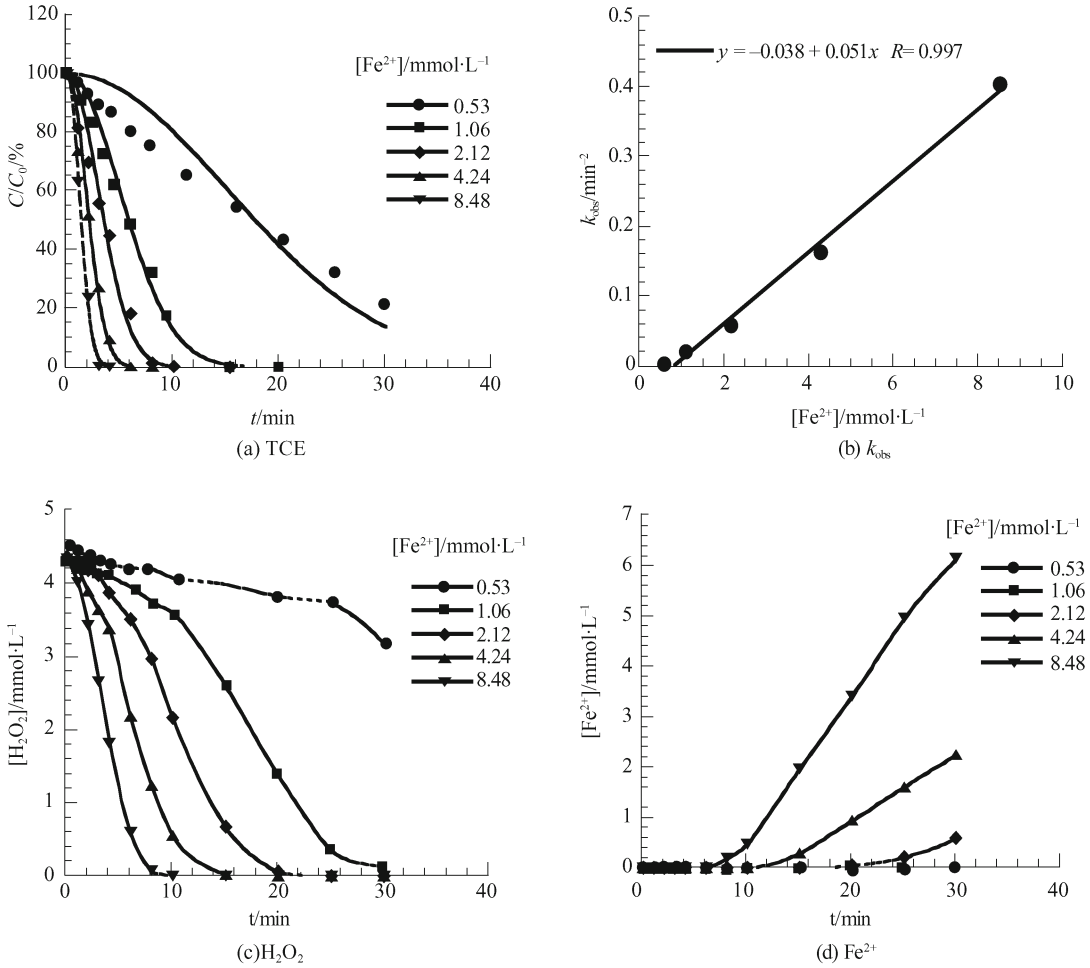


**Fig. 2** Degradation of TCE in pseudo-continuous dosing mode (batch $H_2O_2$ and continuous $Fe^{2+}$). Experimental conditions: $C_{\mathrm{o,TCE}}$ = 0.42–0.46 mmol/L, $[H_2O_2]$ = 4.24 mmol/L

### 3.3 Pseudo-continuous dosing mode

The pseudo-continuous dosing mode with batch $H_2O_2$ and continuous $Fe^{2+}$ was first employed to investigate the degradation of TCE, DCE, and CF with the Fenton's reagent. The results indicate that both TCE and DCE could be completely removed at a sufficient dosage of $Fe^{2+}$ and a total $H_2O_2$ dosage of 4.24 mmol/L (Figs. 2(a) and 3(a)). However, the complete removal of CF seemed impossible despite a high $Fe^{2+}$ concentration (up to 16.96 mmol/L) and an increased $H_2O_2$ dosage (8.48 mmol/L) (Fig. 4(a)). A high $Fe^{2+}$ dosage would not enhance the CF removal but facilitate $Fe^{2+}$ competition for ·OH. The optimal molar ratio ($[H_2O_2]/[Fe^{2+}]$) for the oxidation of CF was about 4:1, which resulted in the highest removal efficiency of 66% (Fig. 4(b)). It is seen that the removal efficiency of selected CAHs highly depends on their molecular structures. Since ·OH is electron-deficient, it prefers to attack the organic compounds with an electron-rich structure such as double-bonds or aromatic-rings. Both TCE and DCE have $SP^2$ hybridized carbon atoms thus, they can be effectively oxidized by ·OH. However, CF only has one $SP^3$ hybridized carbon atom. Moreover, the highly chlorinated feature of CF draws the electrons away from the carbon center. As a result, CF reacts with ·OH more slowly than TCE and DCE.

The results indicate that the "time-squared" kinetic model was applicable for the oxidation of TCE and DCE (Figs. 2(a) and 3(a)), but not for CF due to its low reactivity towards ·OH (Fig. 4(a)). A linear curve could be established between $k_{obs}$ and $Fe^{2+}$ dosage with a slope of 0.051 and 0.035 $min^{-2}$ $(mmol/L)^{-1}$ in the oxidation of TCE and DCE, respectively (Figs. 2(b) and 3(b)). It means that at a fixed $H_2O_2$ dosage, the observed reaction rate increased linearly with the dosage of $Fe^{2+}$. However, there was no linear relationship between $k_{obs}$ and $Fe^{2+}$ dosage in the oxidation of CF since the "time-squared" kinetic model was inapplicable to this reaction system. In comparison with the reaction rate of $Fe^{2+}$ towards ·OH ($3 \times 10^8$ $(mol/L)^{-1}\cdot s^{-1}$), the reaction rates of TCE ($2.9 \times 10^9$ $(mol/L)^{-1}\cdot s^{-1}$) [35] and DCE ($6.8 \times 10^9$

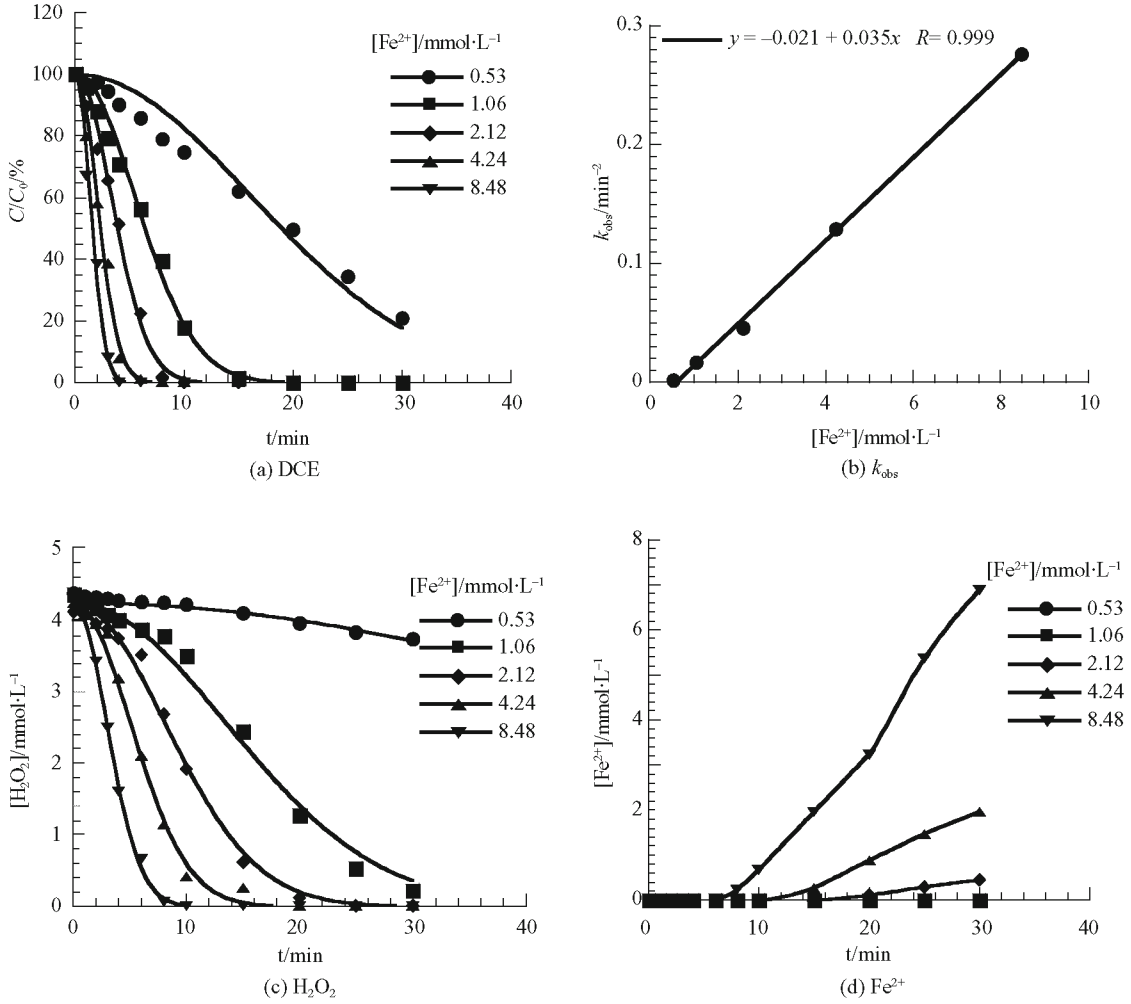


**Fig. 3** Degradation of DCE in pseudo-continuous dosing mode (batch $H_2O_2$ and continuous $Fe^{2+}$). Experimental conditions: $C_{o,DCE} = 0.42$–$0.44$ mmol/L, $[H_2O_2] = 4.24$ mmol/L

$(mol/L)^{-1}\cdot s^{-1}$) [36] towards ·OH are much faster. It implies that the competition from $Fe^{2+}$ for ·OH was insignificant in the oxidation of TCE and DCE. However, the reaction rate of CF towards ·OH is only $5.0 \times 10^7$ $(mol/L)^{-1}\cdot s^{-1}$ [37], much smaller than that of $Fe^{2+}$. It implies that most of ·OH was consumed by $Fe^{2+}$ in the oxidation of CF. When the $Fe^{2+}$ dosage reached an optimal level, further increasing the $Fe^{2+}$ dosage could not enhance the overall removal efficiency but merely increase the initial degradation rate of CF (Fig. 4(a)). Therefore, the prerequisite for application of the "time-squared" kinetic model is that the rate constant of a studied organic comtaminant towards ·OH should be much larger than that of $Fe^{2+}$.

The change of $H_2O_2$ and $Fe^{2+}$ concentrations during the reaction course is shown in Figs. 2c–2d, 3c–3d, and 4c–4d. The results indicate that $H_2O_2$ and $Fe^{2+}$ could not co-exist in the aqueous solution due to a fast reaction between the two chemicals to generate ·OH. If $H_2O_2$ was present in the solution, $Fe^{2+}$ could not be detected. Once $H_2O_2$ was depleted, $Fe^{2+}$ started to appear.

### 3.4 Continuous dosing mode

In the continuous dosing mode, both $H_2O_2$ and $Fe^{2+}$ were continuously added into the reaction system. The degradation of TCE and DCE at a total $H_2O_2$ dosage of 4.24 mmol/L and varied $Fe^{2+}$ dosages (ranging from 0.53 to 8.48 mmol/L) during a reaction course of 30 min is shown in Figs. 5 and 6, respectively. The results indicate that the degradation data of TCE and DCE could be well-fitted by the "time-squared" kinetic model (Figs. 5(a) and 6(a)). Similar to that observed in the above pseudo-continuous dosing mode, a linear curve between $k_{obs}$ and $Fe^{2+}$ dosage could be established with a solpe of 0.0120 and 0.0127 $min^{-2}$ $(mmol/L)^{-1}$ for TCE and DCE, respectively (Figs. 5(b) and 6(b)). For the two chlorinated alkenes, the optimal molar ratio of $[H_2O_2]/[Fe^{2+}]$ was approximately 1:1 because the majority of $H_2O_2$ and $Fe^{2+}$ could be used for organic degradation (Figs. 5(c)–5(d) and 6(c)–6(d)).

Since CF was difficult to degrade due to its highly chlorinated and saturated structure, the dosages of both

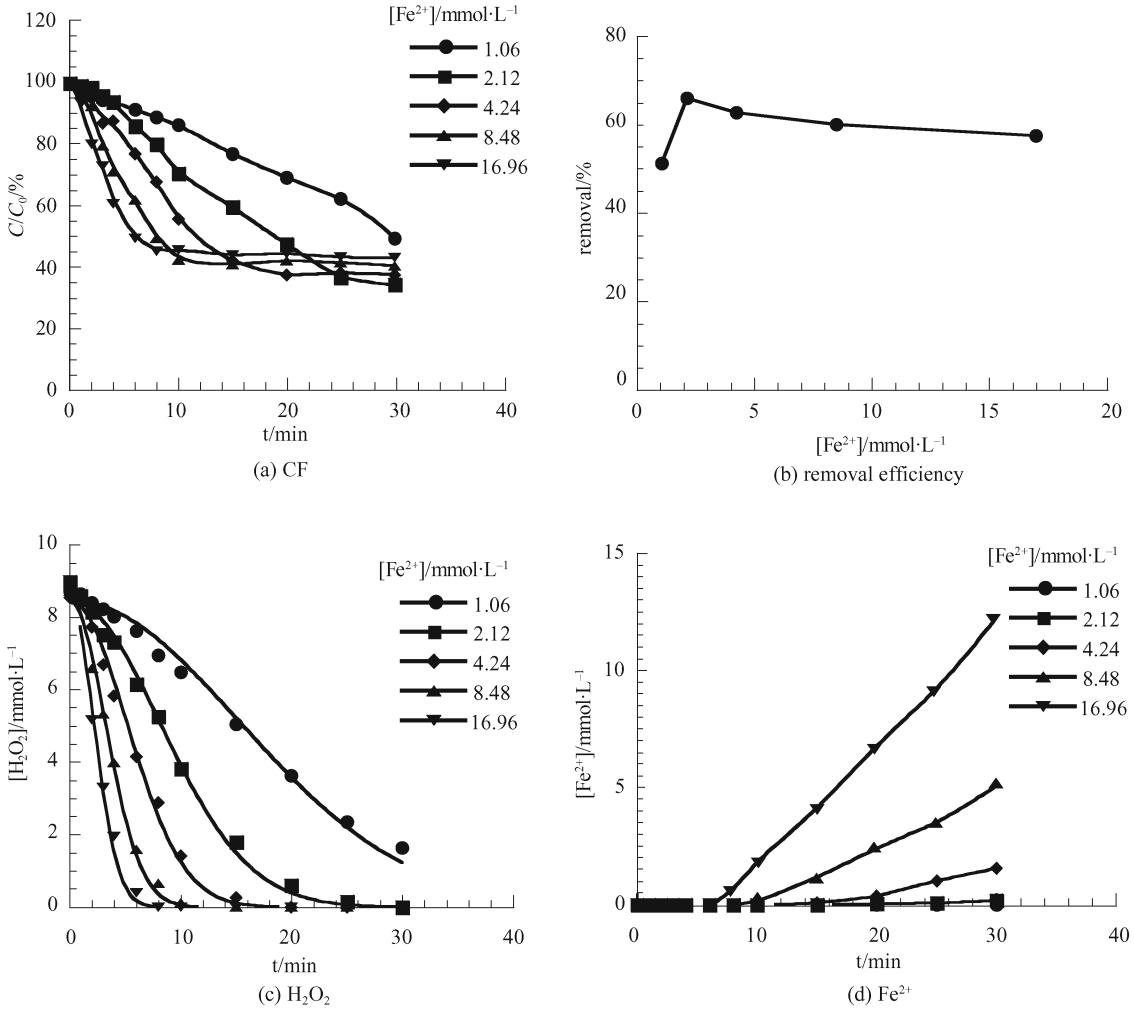


**Fig. 4** Degradation of CF in pseudo-continuous dosing mode (batch $H_2O_2$ and continuous $Fe^{2+}$). Experimental conditions: $C_{o,CF} = 0.43$–$0.47$ mmol/L, $[H_2O_2] = 8.48$ mmol/L

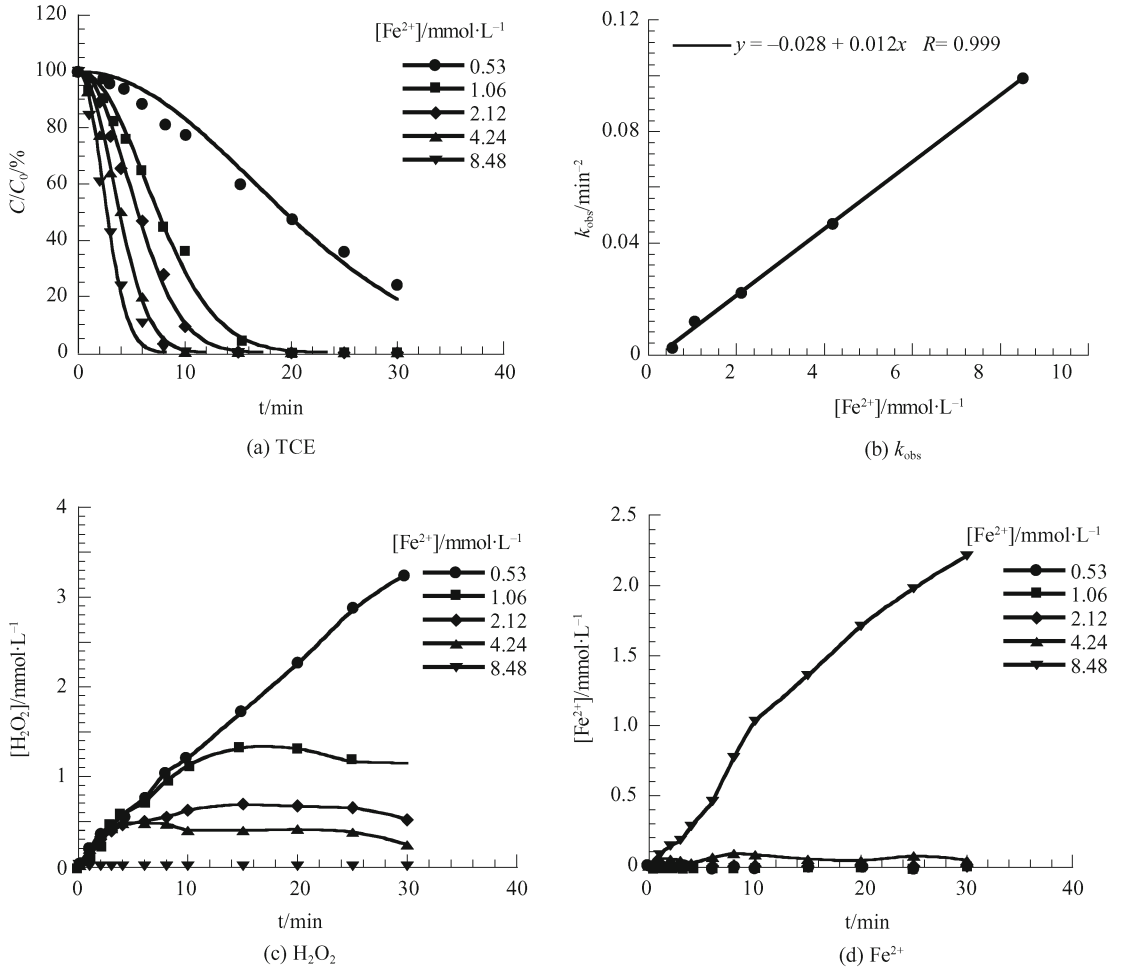


**Fig. 5** Degradation of TCE in continuous dosing mode. Experimental conditions: $C_{o,TCE}$ = 0.43–0.46 mmol/L, $[H_2O_2]$ = 4.24 mmol/L

$H_2O_2$ and $Fe^{2+}$ were doubled. The results indicate that the optimal molar ratio of $[H_2O_2]/[Fe^{2+}]$ was 1:1 (Fig. 7(a)), which led to a maximum removal efficiency of 89% (Fig. 7 (b)). Further increasing the $Fe^{2+}$ dosage would enhance the competition of $Fe^{2+}$ for ·OH, thus decreasing the removal efficiency of CF. At $[Fe^{2+}]$ less than 8.48 mmol/L, $H_2O_2$ accumulated in the reaction solution while $Fe^{2+}$ was not detected. Above this dosage, $Fe^{2+}$ started to accumulate while $H_2O_2$ was depleted (Figs. 7(c)–7(d)). It is particularly noted that most of CF could get removed in the continuous dosing mode although Tang and Huang [25] reported that CF was not degraded in the batch dosing mode. This difference demonstrates that the dosing mode of Fenton's reagent plays an important role in the oxidation of organic compounds, especially for those with $k_{\cdot OH} \leqslant 10^8$ $(mol/L)^{-1}\cdot s^{-1}$. Chen et al. [38] investigated the ultrasonic dechlorination of CF in aqueous solution in the presence of $H_2O_2$. They found that the optimal molar ratio of $[H_2O_2]/[CHCl_3]$ was 50:1 and the highest removal efficiency of CF reached 94%. In our work, a removal efficiency of 89% could be achieved at a significantly decreased molar ratio of $[H_2O_2]/[CHCl_3]$ (20:1) in the continuous dosing mode.

### 3.5 Comparison of different dosing modes

The degradation efficiencies of selected CAHs in different dosing modes are compared in Fig. 8. Three dosing modes were examined in total, namely, batch mode (dosing both $H_2O_2$ and $Fe^{2+}$ in batch), pseudo-continuous mode (dosing either $H_2O_2$ or $Fe^{2+}$ in batch), and continuous mode (dosing both $H_2O_2$ and $Fe^{2+}$ continuously). The results indicate that the removal efficiency primarily depended on the dosing mode of $Fe^{2+}$. When $Fe^{2+}$ was dosed in batch, the organic degradation curves exhibited a similar trend with either batch or continuous dosing of $H_2O_2$. When $Fe^{2+}$ was continuously dosed, the organic degradation curves were also similar with either batch or continuous dosing of $H_2O_2$. This is due to the fact that $Fe^{2+}$ competes for ·OH more strongly than $H_2O_2$, thus varying the dosing mode of $Fe^{2+}$ will greatly affect its inhibition on organic degradation.

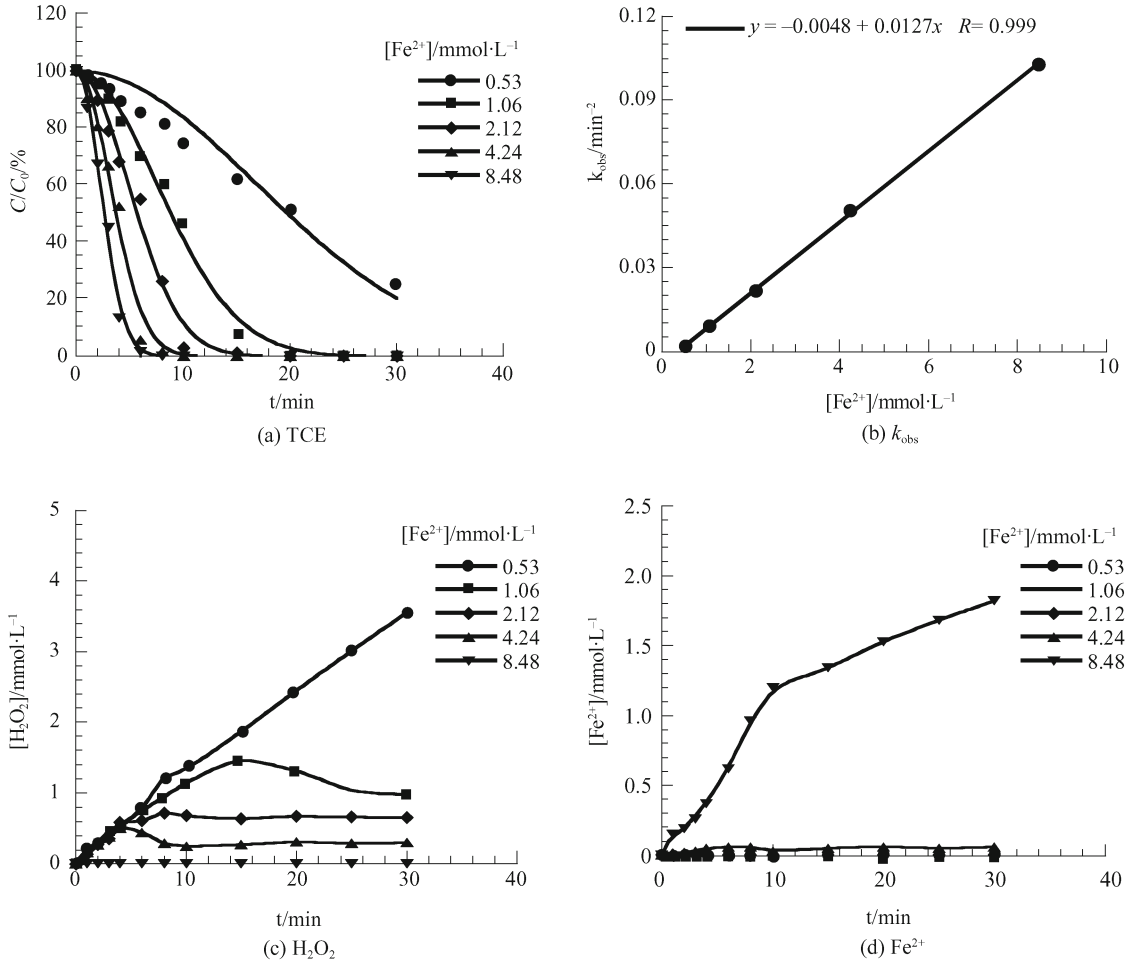


**Fig. 6** Degradation of DCE in continuous dosing mode. Experimental conditions: $C_{o,DCE}$ = 0.42–0.44 mmol/L, $[H_2O_2]$ = 4.24 mmol/L

For the two chlorinated alkenes, the batch-dosing of $H_2O_2$ generally yielded a slightly faster reaction rate than the continuous dosing of $H_2O_2$ despite the dosing mode of $Fe^{2+}$ (Figs. 8(a)–8(b)). A small amount of $Fe^{2+}$ would be regenerated by $H_2O_2$ with a high concentration, as described in Eq. (7) [39]:

$$Fe^{3+} + H_2O_2 \rightarrow Fe^{2+} + HO_2\cdot + H^+. \quad (7)$$

If $H_2O_2$ is dosed in batch, the excessive $H_2O_2$ during the early phase of reaction will promote the partial regeneration of $Fe^{2+}$. If $H_2O_2$ is continuously dosed, the regeneration of $Fe^{2+}$ is insignificant due to a low $H_2O_2$ concentration. Therefore, $Fe^{2+}$ behaves as a "catalyst" only at a high molar ratio of $[H_2O_2]/[Fe^{2+}]$ (e.g., more than 20:1).

However, the continuous dosing of $H_2O_2$ yielded a higher organic removal in the oxidation of CF than the batch dosing of $H_2O_2$ despite the dosing mode of $Fe^{2+}$ (Fig. 8(c)). It is known that CF reacts much more slowly towards ·OH than the chlorinated alkenes. The rate constants of CF and $H_2O_2$ towards ·OH are at the same order of magnitude (i.e., $10^7$ $(mol/L)^{-1}\cdot s^{-1}$). At high concentration $H_2O_2$ will significantly compete for ·OH, thus suppressing the degradation of CF.

To generalize, the pseudo-continuous dosing mode with batch $H_2O_2$ and continuous $Fe^{2+}$ is optimal for the oxidation of chlorinated alkenes ($k_{\cdot OH} > 10^9$ $(mol/L)^{-1}\cdot s^{-1}$), while the continuous mode is optimal for the oxidation of CF ($k_{\cdot OH} < 10^8$ $(mol/L)^{-1}\cdot s^{-1}$).

### 3.6 Degree of dechlorination

The concentration of $Cl^-$ released from the selected CAHs during the oxidation process was monitored to determine the degree of dechlorination. It is the chlorine substituent that mainly accounts for the toxicity of CAHs. Therefore, the degree of dechlorination indirectly represents the degree of detoxification. The results show that at a reaction time of 60 min, the degrees of dechlorination reached 98.5%, 73.2%, and 68.9% for TCE, DCE and CF,

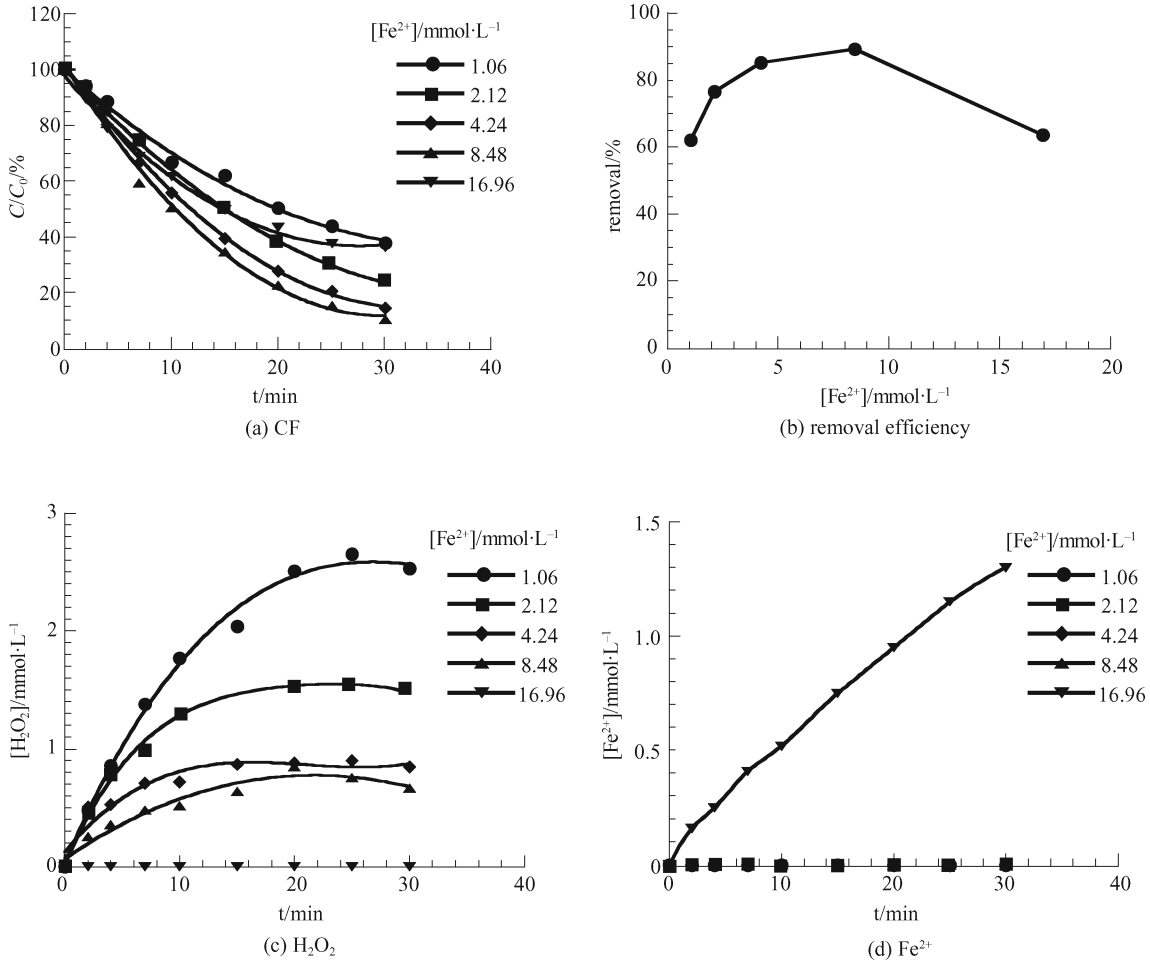


**Fig. 7** Degradation of CF in continuous dosing mode. Experimental conditions: $C_{o,CF}$ = 0.41–0.44 mmol/L, $[H_2O_2]$ = 8.48 mmol/L

respectively (Fig. 9). TCE was most easily dechlorinated among the selected CAHs, exhibiting a nearly complete chloride release. There still remained a considerable amount of partially dechlorinated byproducts (about 30%) in the final solution of DCE and CF, however. Further increasing the dosages of $H_2O_2$ and $Fe^{2+}$ could not notably increase the dechlorination rates of DCE and CF.

### 3.7 Reaction mechanism of TCE with Fenton's reagent

After consecutive extractions of the reaction sample by hexane and MTBE, the MTBE extract was derivatized by diazomethane and analyzed by GC/MS. Identification and quantification of reaction intermediates were based on authentic standards following the same derivatization procedures. The GC/MS chromatogram of the derivatized sample taken at the reaction time of 30 min is shown in Fig. 10a. Only one distinct peak was observed at a retention time of 4.27 min that was identified to be acetic acid-dichloro-methyl ester, the derivatized product of dichloroacetic acid (DCAA). No reaction intermediates were detected during the oxidation of DCE and CF. It is hypothesized that some simple byproducts could be co-eluted with MTBE after diazomethane derivatization and thus were not detected by GC/MS.

Based on the identified intermediate (i.e., DCAA), reaction pathways of TCE degradation are proposed as illustrated in Fig. 10(b). The electron-rich double bond of TCE was first broken upon ·OH attack, forming a carbon-centered radical (T1). This organic radical was highly unstable and after rapid inner-strucutre chlorine rearrangement, a new radical species (T2) was produced. The continuous attack of ·OH and release of HCl led to the generation of DCAA. DCAA could be further mineralized to $CO_2$ and HCl, or partially degraded to other chlorinated and non-chlorinated byproducts.

The evolution of DCAA concentration, which was normalized to the initial concentration of TCE, as a function of reaction time is shown in Fig. 10(c) together with TCE degradation and TOC removal. DCAA started to appear at 5 min, reached its highest concentration of 5.5% at 20 min, and was completely degraded at 60 min. Pignatello et al. [39] reported that the major byproduct

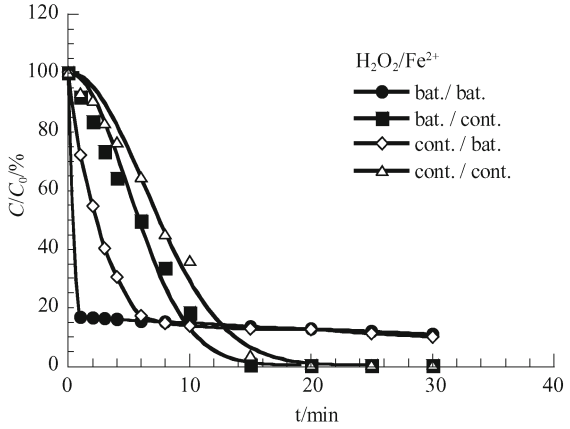


(a) DCE

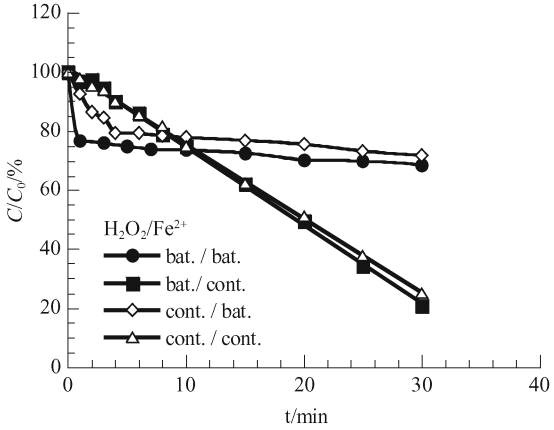


(b) DCE

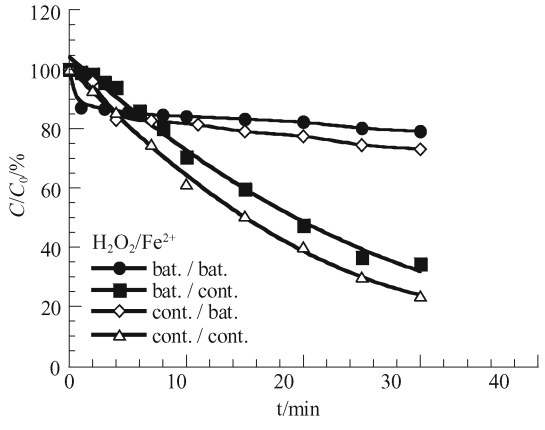


(c) CF

**Fig. 8** Effect of dosing mode on the degradation of selected CAHs. Experimental conditions: $C_{o,TCE}$ = 0.42–0.44 mmol/L, $[H_2O_2]$ = 4.24 mmol/L, $[Fe^{2+}]$ = 1.06 mmol/L; $C_{o,DCE}$ = 0.42–0.44 mmol/L, $[H_2O_2]$ = 4.24 mmol/L, $[Fe^{2+}]$ = 0.53 mmol/L; $C_{o,CF}$ = 0.40–0.45 mmol/L, $[H_2O_2]$ = 8.48 mmol/L, $[Fe^{2+}]$ = 2.12 mmol/L

was DCAA (2.7%) during the oxidation of TCE with a photo-Fenton process. Ollis et al. [19] found that DCAA could be totally mineralized by UV/$TiO_2$. Fig. 10(c) also

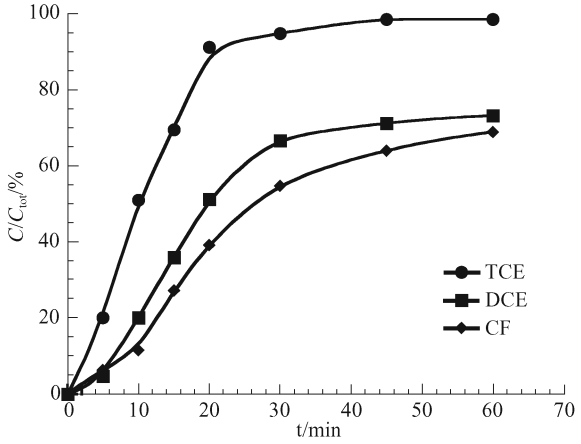


**Fig. 9** Degree of dechlorination in the oxidation of selected CAHs. Experimental conditions: $C_{o,TCE}$ = 0.89 mmol/L, $[H_2O_2] = 1.5 \times 10^{-4}$ mol/L·min$^{-1}$, $[Fe^{2+}] = 7.5 \times 10^{-5}$ mol/L·min$^{-1}$; $C_{o,DCE}$ = 0.98 mmol/L, $[H_2O_2] = 1.5 \times 10^{-4}$ mol/L·min$^{-1}$, $[Fe^{2+}] = 7.5 \times 10^{-5}$ mol/L·min$^{-1}$; $C_{o,CF}$ = 0.97 mmol/L, $[H_2O_2] = 3 \times 10^{-4}$ mol/L·min$^{-1}$, $[Fe^{2+}] = 1.5 \times 10^{-4}$ mol/L·min$^{-1}$

shows that TCE was completely removed at 30 min, and the removal efficiency of TOC reached 76.3% at 60 min. The remaining portion of TOC contained mostly non-chlorinated byproducts since 98.5% of $Cl^-$ could be released from TCE as described above.

## 4 Conclusions

This study investigated the oxidative degradation of three selected CAHs, namely, TCE, DCE and CF, by Fenton's reagent. The degradation efficiency was primarily affected by the molecular structures of the organic contaminants. The chlorinated alkenes (i.e., TCE and DCE) could be readily oxidized by ·OH due to their electron-rich double bond structures. In contrast, CF was difficult to remove due to its highly chlorinated and saturated chemical structure.

The dosing modes of $H_2O_2$ and $Fe^{2+}$ significantly affected the reaction rates of selected CAHs. In particular, the dosing mode of $Fe^{2+}$ played a more important role than that of $H_2O_2$ because $Fe^{2+}$ competed for ·OH more strongly than $H_2O_2$. For the oxidation of TCE and DCE, the experimental data could be well fitted by the proposed "time-squared" kinetic model, i.e., $C = C_o \exp(-k_{obs}t^2)$. For the oxidation of CF, a maximal removal efficiency of 89% could only be achieved in the continuous dosing mode. The degrees of dechlorination reached 98.5%, 73.2%, and 68.9% for TCE, DCE, and CF, respectively.

DCAA was identified to be the major reaction intermediate in the oxidation of TCE, which could be completely removed as the reaction proceeded. No reaction

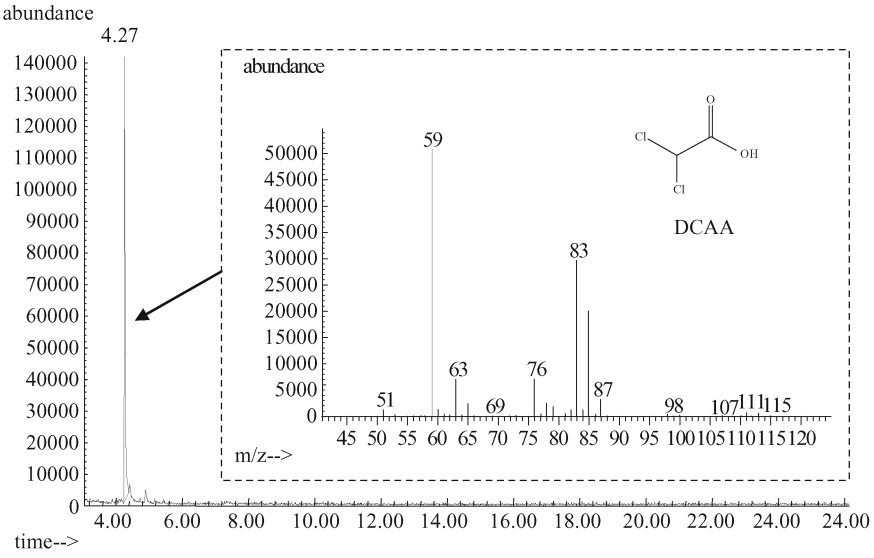


(a) GS/MS chromatogram

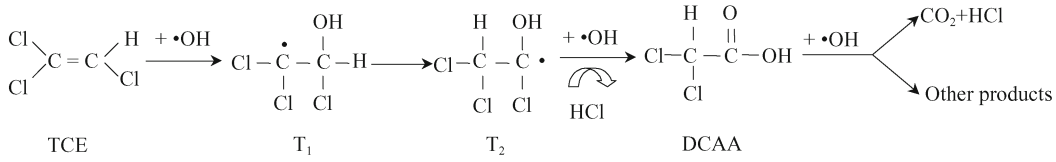


(b) reaction pathways

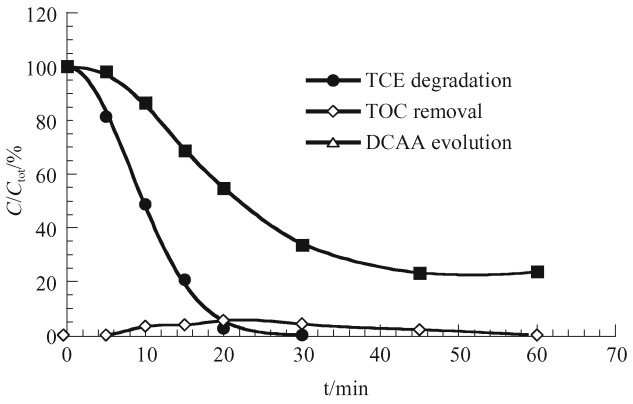


(c) TCE degradation, TOC removal and DCAA evolution

**Fig. 10** Reaction mechanism of TCE with Fenton's reagent. Experimental conditions: $C_{o,TCE} = 0.89$ mmol/L, $[H_2O_2] = 1.5 \times 10^{-4}$ mol/L·min$^{-1}$, $[Fe^{2+}] = 7.5 \times 10^{-5}$ mol/L·min$^{-1}$

intermediates or byproducts were identified in the oxidation of DCE and CF, however.

**Acknowledgements** The authors greatly appreciate the financial support from the Department of Energy, USA (Grant No. DE-FG07-96ER14716). This study was also supported by the National Key Technologies R&D Program funded by the Ministry of Science and Technology of China (Grant No. 2006BAJ08B02).

## References

1. Vogel T M, Criddle C S, McCarty P L. Transformations of halogenated aliphatic compounds: oxidation, reduction, substitution, and dehydrohalogenation reactions occur abiotically or in microbial and mammalian systems. Environmental Science & Technology, 1987, 21(8): 722–736

2. Watts R J. Hazardous Wastes: Sources, Pathways, Receptors. New York: John Wiley & Sons, 1998
3. Higgins T E. Hazardous Waste Minimization Handbook. Chelsea: Lewis Publishers, 1989
4. Mackay D M, Smith L A. Agricultural chemicals in groundwater: Monitoring and management in California. Journal of Soil and Water Conservation, 1990, 45(2): 253–255
5. ATSDR Biannual Report to Congress (10/17/1986–9/30/1988). Agency for Toxic Substances and Disease Registry, U.S. Public Health Service, Atlanta, GA, 1989
6. Keith L H, Telliard W A. Priority pollutants I-a perspective view. Environmental Science & Technology, 1979, 13(4): 416–423
7. El-Farhan Y H, Scow K M, de Jonge L W, Rolston D E, Moldrup P. Coupling transport and biodegradation of toluene and trichloroethylene in unsaturated soils. Water Resources Research, 1998, 34(3): 437–445
8. Heron G, Van Zutphen M, Christensen T H, Enfield C G. Soil heating for enhanced remediation of chlorinated solvents: a laboratory study on resistive heating and vapor extraction in a silty, low-permeable soil contaminated with trichloroethylene. Environmental Science & Technology, 1998, 32(10): 1474–1481
9. Kawala Z, Atamanczuk T. Microwave-enhanced thermal decontamination of soil. Environmental Science & Technology, 1998, 32(17): 2602–2607
10. Huang C P, Dong C D, Tang Z H. Advanced chemical oxidation: Its present role and future potential in hazardous waste treatment. Waste Management, 1993, 13(5/7): 361–377
11. Burris D R, Delcomyn C A, Deng B L, Buck L E, Hatfield K. Kinetics of tetrachloroethylene-reductive dechlorination catalyzed by vitamin $B_{12}$. Environmental Toxicology and Chemistry, 1998, 17(9): 1681–1688
12. Ho S V, Athmer C, Sheridan P W, Hughes B M, Orth R, McKenzie D, Brodsky P H, Shapiro A, Thornton R, Salvo J, Schultz D, Landis R, Griffith R, Shoemaker S. The lasagna technology for in situ soil remediation. 1. Small field test. Environmental Science & Technology, 1999, 33(7): 1086–1091
13. Ho S V, Athmer C, Sheridan P W, Hughes B M, Orth R, McKenzie D, Brodsky P H, Shapiro A, Sivaves T M, Salvo J, Schultz D, Landis R, Griffith R, Shoemaker S. The lasagna technology for in situ soil remediation. 2. Large field test. Environmental Science & Technology, 1999, 33(7): 1092–1099
14. Gotpagar J, Grulke E, Tsang T, Bhattacharyya D. Reductive dehalogenation of trichloroethylene using zero-valent iron. Environmental Progress, 1997, 16(2): 137–143
15. Arnold W A, Roberts A L. Pathways of chlorinated ethylene and chlorinated acetylene reaction with Zn (0). Environmental Science & Technology, 1998, 32(19): 3017–3025
16. Cooper W J, Meacham D E, Nickelsen M G, Lin K, Ford D B, Kurucz C N, Waite T D. The removal of trichloroethylene (TCE) and tetrachloroethylene (PCE) from aqueous-solution using high-energy electrons. Journal of the Air & Waste Management Association, 1993, 43(10): 1358–1366
17. Bhatnagar A, Cheung H M. Sonochemical destruction of chlorinated C1 and C2 volatile organic compounds in dilute aqueous solution. Environmental Science & Technology, 1994, 28(8): 1481–1486
18. Crittenden J C, Liu J, Hand D W, Perram D L. Photocatalytic oxidation of chlorinated hydrocarbons in water. Water Research, 1997, 31(3): 429–438
19. Ollis D F, Hsiao C Y, Budiman L, Lee C L. Heterogeneous photoassisted catalysis: conversions of perchloroethylene, dichloroethane, chloroacetic acids, and chlorobenzenes. Journal of Catalysis, 1984, 88(1): 89–96
20. Amama P B, Itoh K, Murabayashi M. Effect of $RuO_2$ deposition on the activity of $TiO_2$: Photocatalytic oxidation of trichloroethylene in aqueous phase. Journal of Materials Science, 2004, 39: 4349–4351
21. Glaze W H, Kenneke J F, Ferry J L. Chlorinated byproducts from the $TiO_2$-mediated photodegradation of trichloroethylene and tetrachloroethylene in water. Environmental Science & Technology, 1993, 27(1): 177–184
22. Bull R J, Sanchez I M, Nelson M A, Larson J L, Lansing A J. Liver tumor induction in B6C3F1 mice by dichloroacetate and trichloroacetate. Toxicology, 1990, 63(3): 341–359
23. Ravikumar J X, Gurol M D. Chemical oxidation of chlorinated organics by hydrogen peroxide in the presence of sand. Environmental Science & Technology, 1994, 28(3): 394–400
24. Chen G, Hoag G E, Chedda P, Nadim F, Woody B A, Dobbs G M. The mechanism and applicability of in situ oxidation of trichloroethylene with Fenton's reagent. Journal of Hazardous Materials, 2001, B87: 171–186
25. Tang W Z, Huang C P. Stoichiometry of Fenton's reagent in the oxidation of chlorinated aliphatic organic pollutants. Environmental Technology, 1997, 18(1): 13–23
26. Tang W Z, Tassos S. Oxidation kinetics and mechanisms of trihalomethanes by Fenton's reagent. Water Research, 1997, 31(5): 1117–1125
27. Liang C, Bruell C J. Thermally activated persulfate oxidation of trichloroethylene: Experimental investigation of reaction orders. Industrial Engineering Chemical Research, 2008, 47: 2912–2918
28. Schwarzenbach R P, Gschwend P M, Imboden D M. Environmental Organic Chemistry. New York: John Wiley & Sons, 1993
29. Fales H M, Jaouni T M, Babashak J F. Simple device for preparing ethereal diazomethane without resorting to codistillation. Analytical Chemistry, 1973, 45(13): 2302–2303
30. Knapp D R. Handbook of Analytical Derivatization Reactions. New York: John Wiley & Sons, 1979
31. Qiang Z M, Chang J H, Huang C P, Cha D. Oxidation of selected polycyclic aromatic hydrocarbons by the Fenton's reagent: effect of major factors including organic solvent. In: Heineman W R, Eller P G, eds. Nuclear Site Remediation: First Accomplishments of the Environmental Management Science Program. Washington, DC: American Chemical Society, 2000, 187–209
32. Walling C. Fenton's reagent revisited. Accounts of Chemical Research, 1975, 8: 125–131
33. Sedlak D L, Andren A W. Oxidation of chlorobenzene with Fenton's reagent. Environmental Science & Technology, 1991, 25(4): 777–782
34. Beltran F J, Gonzalez M, Rivas F J, Alvarez P. Fenton reagent advanced oxidation of polynuclear aromatic hydrocarbons in water. Water Air & Soil Pollution, 1998, 105(3–4): 685–700
35. Getoff N. Radiation-degradation and photoinduced-degradation of pollutants in water—A comparative-study. Radiation Physics and Chemistry, 1991, 37(5–6): 673–680
36. Köster R, Asmus K D. Die Reaktionen chlorierter Äthylene mit hydrotisierten Elektronen und OH-Radikalen in wässriger Lösung. Z. Naturforsch, 1971, 26b: 1108–1116
37. Haag W R, Yao C C D. Rate constants for reaction of hydroxyl radicals with several drinking-water contaminants. Environmental Science & Technology, 1992, 26(5): 1005–1013
38. Chen J R, Xu X W, Lee A S, Yen T F. A feasibility study of dechlorination of chloroform in water by ultrasound in the presence of hydrogen peroxide. Environmental Technology, 1990, 11(9): 829–836
39. Pignatello J J, Liu D, Huston P. Evidence for an additional oxidant in the photoassisted Fenton reaction. Environmental Science & Technology, 1999, 33(11): 1832–1839